Paweł SZCZEŚNIAK[1]
Zbigniew FEDYCZAK[1]

MODELLING AND ANALYSIS OF MATRIX-REACTANCE FREQUENCY CONVERTER BASED ON ĆUK TOPOLOGY BY DQ0 TRANSFORMATION

This paper deals with a three-phase direct matrix-reactance frequency converter (MRFC) with Ćuk topology and includes a description of its topology and operation plus presentation of the results of an investigation of its properties. The static and dynamic characteristics of the presented converter under the control strategy proposed by Venturini are fully analysed based on the basis of the circuit models development by the circuit DQ0 transformation. Various static converter characteristics such as voltage and current gain, phase of voltage transmittance and power factor are completely analysed. Transition characteristics are also analysed by a small-signal model. The usefulness of the models is verified through computer simulations with good agreements.

1 INTRODUCTION

In recent years, the direct matrix converters have received considerable attention as a competitor to the normally-used pulse width-modulated voltage-source inverter (PWM-VSI). The real development of MC starts with work of [1]. As it is well known, the MC, compared to the PWM-VSI with diode rectification stage at the input provides sinusoidal input and output waveforms, bidirectional power flow, controllable input power factor, and more compact design [1]-[6]. One disadvantage of the MC is the voltage transfer ratio, which is limited to 0.5 of the input voltage [1] at linear voltage transformation, and to 0.866 or 1.053 at low-frequency load voltage deformations for space-vector or fictitious DC link control strategy concepts respectively [2]-[6]. In research [7] and [8] the general conception of a three-phase direct MRFC with buck-boost output voltage is presented, whereas in research [9] and [10], the conception of MRFC with Ćuk topology was presented. The topology of this MRFC is based on matrix reactance choppers (MRC) with load switches arranged as in MC. Such an approach gives the possibility to obtain a load output voltage greater than the input one.

In this paper we obtained the analytic expressions for the voltage and current gain, input power factor and phase of voltage transmittance of the MRFC based with Ćuk

[1] University of Zielona Gora, Instytut Institute of Electrical Engineering
Podgórna 50 Str., 65-246 Zielona Góra, Poland, +48 68 328 25 38
P.Szczesniak@iee.uz.zgora.pl, Z.Fedyczak@iee.uz.zgora.pl

topology, using DQ0 transformation technique [11]-[14]. By applying the circuit DQ0 transformation, the three-phase-balanced MRFC is transformed into a simple single-phase circuit that does not contain a switch element. The switches are transformed to equivalent transformers whereas voltage sources and passive components are transformed into equivalent components.

2 DESCRIPTION OF PRESENTED SOLUTION

The schematic diagram of the main circuit of the presented MRFC is shown in Fig. 1a [9], [10]. In this circuit a three-phase Ćuk MRC with load switches arranged as in MC is used. A description of the control strategy of the MRFC, in general form, is illustrated in Fig. 1b. In each switching period T_S, in the time t_S (switching time of the source switches S_{jk}, where j={a, b, c} is the name of the output phase, k={A, B, C} is the name of the input phase), 3 of 9 matrix switches, S_{ak}, S_{bk}, S_{ck}, are simultaneously closed and all source switches S_{S1}, S_{S2}, S_{S3} are closed at the same time. In time t_L load switches S_{S1}, S_{S2}, S_{S3} are opened and all matrix switches are closed. A simplified view of the control strategy realization is depicted in Fig. 1c.

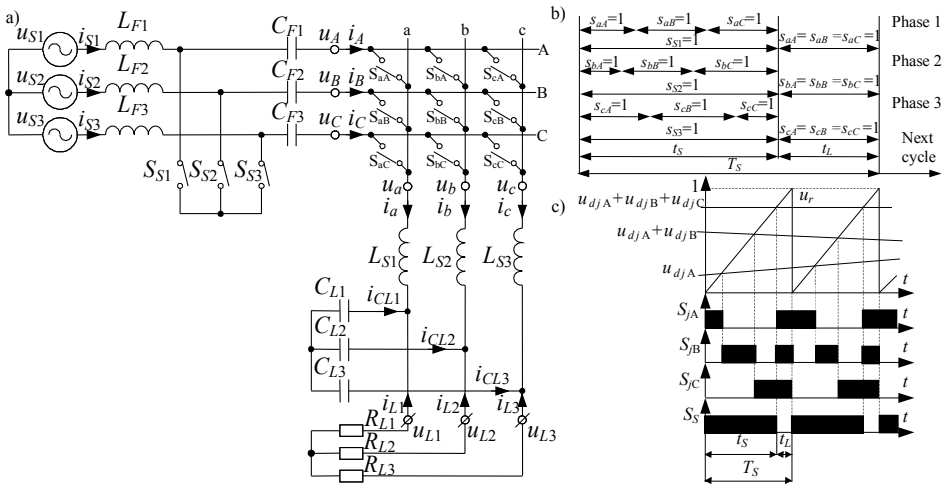

Fig. 1. The MRFC with Ćuk topology a) schematic diagram of main circuit, b) general form of control strategy description, c) exemplary time waveforms of the control signals for switches in one phase

Let the state function of the source switches be defined as (1) and assume that allowed constraints of the source switches in the time t_S is expressed by (2), only 27 out of 2^9 work states of these switches are valid in this time t_S, similarly as in the MC [1]-[6]. In a full switching period, in the time T_S, (27+1) work states can occur in the presented circuit.

$$s_{jk} = \begin{cases} 1, & S_{kj} \text{ on} \\ 0, & S_{kj} \text{ off} \end{cases}, \qquad (1)$$

$$s_{jA} + s_{jB} + s_{jC} = 1 . \qquad (2)$$

Furthermore, on the basis of a classical control strategy [1] attributable to Venturini, assume that there will be realized a control strategy making allowances for changes in the pulse duty factor of the source switch state function s_{jk} expressed by:

$$\mathbf{D} = \frac{1}{3} D_j \begin{bmatrix} 1+2q\cos(\omega_m t) & 1+2q\cos(\omega_m t-2\pi/3) & 1+2q\cos(\omega_m t-4\pi/3) \\ 1+2q\cos(\omega_m t-4\pi/3) & 1+2q\cos(\omega_m t) & 1+2q\cos(\omega_m t-2\pi/3) \\ 1+2q\cos(\omega_m t-2\pi/3) & 1+2q\cos(\omega_m t-4\pi/3) & 1+2q\cos(\omega_m t) \end{bmatrix}, \quad (3)$$

where $D_j=d_{jA}+d_{jB}+d_{jC}=t_S/T_S$ is the summarized pulse duty factor, $q = U_{jm}/U_{Sjm}$ - voltage gain of the source switches set S_{jk} ($0 < q \le 0.5$), $\omega_m = \omega_L - \omega_S$ - setting value of difference between pulsations of the output and supply voltages.

3 CIRCUIT DQ0 TRANSFORMATION

Sinusoidal time-varying systems can be changed to time-invariant system by the DQ0 transformation [11]-[14]. The DQ0 transformation of the variables is given as follows:

$$\begin{aligned} \mathbf{x}_{abc} &= \mathbf{K}\mathbf{x}_{dq0} \\ \mathbf{x}_{dq0} &= \mathbf{K}^{-1}\mathbf{x}_{abc} \end{aligned}, \quad (4) \quad \mathbf{K} = \sqrt{\frac{2}{3}} \begin{bmatrix} \cos(\omega t) & \cos(\omega t-2\pi/3) & \cos(\omega t+2\pi/3) \\ \sin(\omega t) & \sin(\omega t-2\pi/3) & \sin(\omega t+2\pi/3) \\ 1/\sqrt{2} & 1/\sqrt{2} & 1/\sqrt{2} \end{bmatrix}, \quad (5)$$

where: $\mathbf{x}_{abc}=[x_a, x_b, x_c]^T$, $\mathbf{x}_{qd0}=[x_q, x_d, x_0]^T$, x_q- forward (roating) phasor, x_d- backwadr (roating) phasor, x_0- zero-sequence component.

The circuit DQ0 transformation is obtained by the following procedures:

1) Partition of the circuit into basic subcircuits.
2) Transformation of each of the subcircuits into DQ0 equivalent circuits based on the DQ0 transformation equations
3) Reconstruction of the transformed subcircuits by connecting the nodes of adjacent subcircuits.

We can divide the presented MRFC based on Ćuk topology depicted in Fig.1 into several fundamental subcircuits along the dotted lines indicated in Fig.2. After partitioning, we obtain eight subscircuits. As in the presented topology, there are two input and output work frequencies, we also have two transform matrix $\mathbf{K}_S$ and $\mathbf{K}_L$ expressed by (6) and (7) [15], [16].

$$\mathbf{K}_S = \sqrt{\frac{2}{3}} \begin{bmatrix} \cos(\omega_S t) & \cos(\omega_S t-2\pi/3) & \cos(\omega_S t+2\pi/3) \\ \sin(\omega_S t) & \sin(\omega_S t-2\pi/3) & \sin(\omega_S t+2\pi/3) \\ 1/\sqrt{2} & 1/\sqrt{2} & 1/\sqrt{2} \end{bmatrix}, \quad (6)$$

$$\mathbf{K}_L = \sqrt{\frac{2}{3}} \begin{bmatrix} \cos(\omega_L t) & \cos(\omega_L t-2\pi/3) & \cos(\omega_L t+2\pi/3) \\ \sin(\omega_L t) & \sin(\omega_L t-2\pi/3) & \sin(\omega_L t+2\pi/3) \\ 1/\sqrt{2} & 1/\sqrt{2} & 1/\sqrt{2} \end{bmatrix}. \quad (7)$$

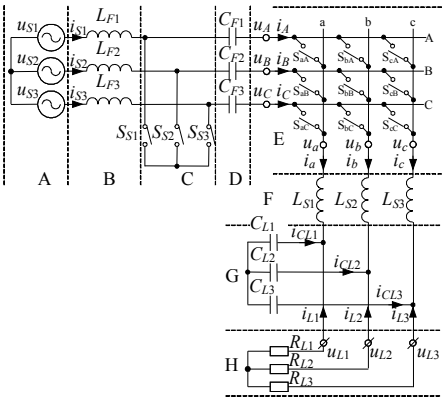

Fig. 2. Partitioning of MRFC for DQ0 transforms

For three-phase balanced voltage sources set (Part A), the DQ0 transformation procedure is as follows:

$$\mathbf{u}_{Sqd0} = \mathbf{K}_S \mathbf{u}_S = \mathbf{K}_S U_S \sqrt{\frac{2}{3}} \begin{bmatrix} \sin(\omega t + \varphi_1) \\ \sin(\omega t - 2\pi/3 + \varphi_1) \\ \sin(\omega t + 2\pi/3 + \varphi_1) \end{bmatrix} = U_S \begin{bmatrix} \sin\varphi_1 \\ \cos\varphi_1 \\ 0 \end{bmatrix}, \tag{8}$$

where $\mathbf{u}_S$ is the vector of the voltage sources. Thus, the DQ0 transformed circuits of voltage sources set is shown in Fig. 3a.

Using basic principles from circuit theory, the source and load inductors (Part B and Part F) are modelled by equation (9) and (10):

$$L_F \dot{\mathbf{i}}_{LFabc} = \mathbf{u}_{LFabc}, \tag{9}$$

$$L_S \dot{\mathbf{i}}_{LSabc} = \mathbf{u}_{LSabc}, \tag{10}$$

where $L_{F1}=L_{F2}=L_{F3}=L_F$, $L_{S1}=L_{S2}=L_{S3}=L_S$. Application of (4)-(7) to (9) and (10) the DQ0 transform of inductors can be formulated as:

$$L_F \left(\dot{\mathbf{K}}_S^{-1} \mathbf{i}_{LFqd0} + \mathbf{K}_S^{-1} \dot{\mathbf{i}}_{LFqd0} \right) = \mathbf{u}_{LFabc}, \tag{11}$$

$$L_S \left(\dot{\mathbf{K}}_L^{-1} \mathbf{i}_{LSqd0} + \mathbf{K}_L^{-1} \dot{\mathbf{i}}_{LSqd0} \right) = \mathbf{u}_{LSabc}, \tag{12}$$

$$L_F \dot{\mathbf{i}}_{LFqd0} = -L_F \mathbf{K}_S \left(\dot{\mathbf{K}}_S^{-1} \right) \mathbf{i}_{LFqd0} + \mathbf{K}_S \mathbf{u}_{LFqd0} = -L_F \omega_S \begin{bmatrix} 0 & 1 & 0 \\ -1 & 0 & 0 \\ 0 & 0 & 0 \end{bmatrix} \mathbf{i}_{LFqd0} + \mathbf{u}_{LFqd0}, \tag{13}$$

$$L_S \dot{\mathbf{i}}_{LSqd0} = -L_S \mathbf{K}_L \left(\dot{\mathbf{K}}_L^{-1} \right) \mathbf{i}_{LSqd0} + \mathbf{K}_L \mathbf{u}_{LSqd0} = -L_S \omega_L \begin{bmatrix} 0 & 1 & 0 \\ -1 & 0 & 0 \\ 0 & 0 & 0 \end{bmatrix} \mathbf{i}_{LSqd0} + \mathbf{u}_{LSqd0}. \tag{14}$$

The circuit models are shown in Fig. 3b and Fig. 3c. The DQ0 "inductor" by real dynamic inductor L_F (L_S) in series with an imaginary static reactor $\pm j\omega_S L_F$ ($\pm j\omega_L L_S$) is represented. Since the voltage and current of the static reactor obeys Ohm's law, the reactor is replaced by a lossless resistor symbol.

For the source and load capacitors circuit (Part D and Part G), the differential equations are in the following form:

$$C_F \dot{\mathbf{u}}_{CFabc} = \mathbf{i}_{CFabc}, \qquad (15) \qquad C_L \dot{\mathbf{u}}_{CLabc} = \mathbf{i}_{CLabc}, \qquad (16)$$

where $C_{F1}=C_{F2}=C_{F3}=C_F$, $C_{L1}=C_{L2}=C_{L3}=C_L$. Taking into account expressions (4)-(7) and (15), (16) the DQ0 transform of source and load capacitors is defined as follows:

$$C_F\left(\dot{\mathbf{K}}_S^{-1}\mathbf{u}_{CFqd0} + \mathbf{K}_S^{-1}\dot{\mathbf{u}}_{CFqd0}\right) = \mathbf{i}_{CFabc}, \quad (17) \qquad C_L\left(\dot{\mathbf{K}}_L^{-1}\mathbf{u}_{CLqd0} + \mathbf{K}_L^{-1}\dot{\mathbf{u}}_{CLqd0}\right) = \mathbf{i}_{CLabc}, \quad (18)$$

$$C_F\dot{\mathbf{u}}_{CFqd0} = -C_F\omega_S\begin{bmatrix}0 & 1 & 0\\ -1 & 0 & 0\\ 0 & 0 & 0\end{bmatrix}\mathbf{u}_{CFqd0} + i_{CFqd0}, \quad (19) \qquad C_L\dot{\mathbf{u}}_{CLqd0} = -C_L\omega_L\begin{bmatrix}0 & 1 & 0\\ -1 & 0 & 0\\ 0 & 0 & 0\end{bmatrix}\mathbf{u}_{CLqd0} + i_{CLqd0}. \quad (20)$$

The DQ0 transformed circuit of source and load capacitors sets are shown in Fig. 3d and Fig. 3e, respectively. Similar as with inductors, the DQ0 "capacitors" are represented by real dynamic capacitors C_F and C_L parallel with an imaginary static reactors $\pm 1/(j\omega_S C_F)$, and $\pm 1/(j\omega_L C_L)$.

Assuming that, $R_{L1}=R_{L2}=R_{L3}=R_L$, the procedure of DQ0 transform of the resistor set (Part H) is as follows (Fig. 3f):

$$\mathbf{u}_{Lqd0} = \mathbf{K}_L\mathbf{u}_{Labc} = \mathbf{K}_L R_L\mathbf{i}_{Lqd0} = R_L\mathbf{i}_{Lqd0}. \qquad (21)$$

If, the switching function of source switches (Part C) are defined by (22), then the DQ0 transform of this switches is described as (23) (Fig. 3h):

$$\mathbf{D}_1 = \begin{bmatrix}(1-D_j) & 0 & 0\\ 0 & (1-D_j) & 0\\ 0 & 0 & (1-D_j)\end{bmatrix}, \quad (22) \qquad \begin{aligned}&\mathbf{u}_{Sabc} = \mathbf{D}_1\mathbf{u}_{Labc}\\ &\mathbf{K}_S\mathbf{u}_{Sqd0} = \mathbf{D}_1\mathbf{K}_S\mathbf{u}_{Lqd0}\\ &\mathbf{u}_{Sqd0} = \mathbf{D}_1\mathbf{u}_{Lqd0}\end{aligned}. \quad (23)$$

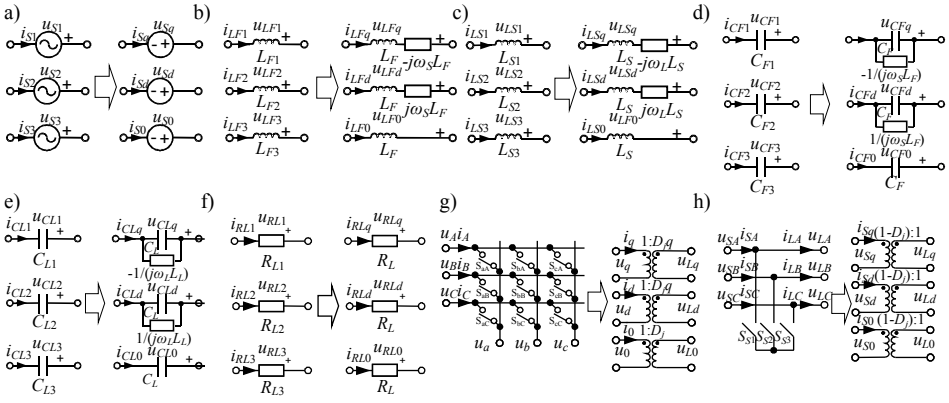

Fig. 3. DQ0 transformation of: a) source voltages, b) source inductors, c) load inductors, d) source capacitors, e) load capacitors, f) load resistors, g) matrix switches, h) sources switches

If, the switching function of matrix switches is defined by (3) then the DQ0 transformation of the nine-switch matrix (Part E) is given as follows [15]-[16] (Fig. 3g):

$$\mathbf{u}_{Sqd0} = \mathbf{K}_S\mathbf{u}_{Sabc} = \mathbf{K}_S\mathbf{D}_{abc}\mathbf{u}_{Labc} = \mathbf{K}_S\mathbf{D}_{abc}\mathbf{K}_L\mathbf{u}_{Lqd0} = \mathbf{D}_{dq0}\mathbf{u}_{Lqd0}\,, \tag{24}$$

$$\mathbf{D}_{qd0} = \mathbf{K}_S\mathbf{D}_{abc}\mathbf{K}_L = D_j\begin{bmatrix} q & 0 & 0 \\ 0 & q & 0 \\ 0 & 0 & 1 \end{bmatrix}. \tag{25}$$

The equivalent DQ0 circuit models of the presented MRFC witch Ćuk topology (Fig. 1) are obtained as shown in Fig. 4 by rejoining of the DQ0 transformed subcircuits. Therefore, the three-phase circuit in Fig. 1 can be represented by three single-phase subcircuits for forward, backward and zero-sequence component.

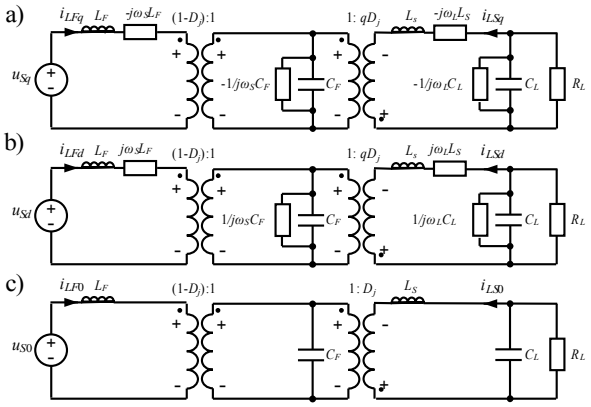

Fig. 4. DQ0 transformation of three phase MRFC based on Ćuk topology, a) forward sequence component, b) backward sequence component, c) zero-sequence component

Furthermore, assuming that initial phase of input voltages equal zero $\varphi_1=0$ and symmetrical balanced three-phase circuit we obtain [11]-[16]:

$$\mathbf{u}_{Sqd0} = \mathbf{K}_S\mathbf{u}_S = U_S\begin{bmatrix} 0 \\ 1 \\ 0 \end{bmatrix}. \tag{26}$$

The equivalent circuits have been simplified from three circuits to one circuit, which is shown in Fig. 5.

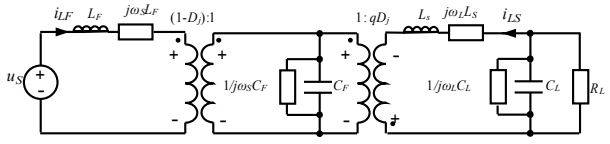

Fig. 5. DQ0 transformation of three phase MRFC based on Ćuk topology (Fig. 1) for $\varphi_1=0$, and balanced-symmetrical circuit condition

4 STEADY STATE ANALYSIS

The steady state model is obtained simply by eliminating the reactive elements. The inductors seem to be short and capacitors open, shown in Fig. 6. The steady state characteristics can be obtained by considering the circuit model of the presented MRFC. For steady state analysis a single-phase circuit model is divided into four terminal networks (Fig. 6) [8], [17]. With reference to Fig. 6 four-terminal chain equations in complex form can be written as (27)-(32).

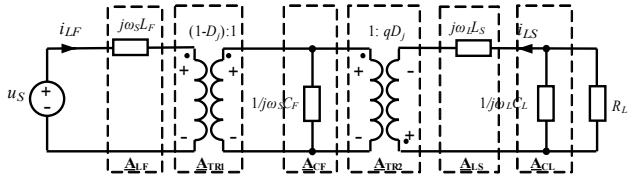

Fig. 6. Steady state equivalent circuit for MRFC with Ćuk topology; $\underline{\boldsymbol{A}}_{LF}$, $\underline{\boldsymbol{A}}_{LS}$ chain matrix for the source and load inductors respectively, $\underline{\boldsymbol{A}}_{TR1}$, $\underline{\boldsymbol{A}}_{TR2}$ chain matrix for source and load transformer respectively, $\underline{\boldsymbol{A}}_{CF}$, $\underline{\boldsymbol{A}}_{CL}$ chain matrix for the source and load capacitors respectively

$$\underline{\mathbf{A}}_{\mathbf{LF}} = \begin{bmatrix} 1 & jL_F\omega_S \\ 0 & 1 \end{bmatrix}, \quad (27) \qquad \underline{\mathbf{A}}_{\mathbf{LS}} = \begin{bmatrix} 1 & jL_S\omega_L \\ 0 & 1 \end{bmatrix}, \quad (28) \qquad \underline{\mathbf{A}}_{\mathbf{CF}} = \begin{bmatrix} 1 & 0 \\ jC_F\omega_S & 1 \end{bmatrix}, \quad (29)$$

$$\underline{\mathbf{A}}_{\mathbf{CL}} = \begin{bmatrix} 1 & 0 \\ jC_L\omega_L & 1 \end{bmatrix}, (30) \quad \underline{\mathbf{A}}_{\mathbf{TR1}} = \begin{bmatrix} (1-D_j) & 0 \\ 0 & \dfrac{1}{(1-D_j)} \end{bmatrix}, (31) \quad \underline{\mathbf{A}}_{\mathbf{TR2}} = \begin{bmatrix} -\dfrac{1}{qD_j} & 0 \\ 0 & -qD_j \end{bmatrix}. (32)$$

Applying the four-terminal network description method [8], [17], [18] we obtain:

$$\begin{bmatrix} \underline{U}_S \\ \underline{I}_S \end{bmatrix} = \underline{\mathbf{A}} \begin{bmatrix} \underline{U}_L \\ \underline{I}_L \end{bmatrix} = \begin{bmatrix} \underline{A}_{11} & \underline{A}_{12} \\ \underline{A}_{21} & \underline{A}_{22} \end{bmatrix} \begin{bmatrix} \underline{U}_L \\ \underline{I}_L \end{bmatrix}, \quad (33) \qquad \underline{\mathbf{A}} = \underline{\mathbf{A}}_{\mathbf{LF}}\underline{\mathbf{A}}_{\mathbf{TR1}}\underline{\mathbf{A}}_{\mathbf{CF}}\underline{\mathbf{A}}_{\mathbf{TR2}}\underline{\mathbf{A}}_{\mathbf{LS}}\underline{\mathbf{A}}_{\mathbf{CL}}. \quad (34)$$

$$\underline{\mathbf{A}} = \begin{bmatrix} \dfrac{(1-D_j)^2\left(C_L L_L\omega_L^2 - 1\right) + L_F\omega_S\left(C_F\omega_S + C_L\omega_L\left(q^2D_j^2 - C_F L_L\omega_S\omega_L\right)\right)}{q(1-D_j)D_j} & \dfrac{-j\left((1-D_j)^2 L_L\omega_L + L_F\omega_S\left(q^2D_j^2 - C_F L_L\omega_S\omega_L\right)\right)}{q(1-D_j)D_j} \\ -\dfrac{j\left(C_F\omega_S + C_L\omega_L\left(q^2D_j^2 - C_F L_L\omega_S\omega_L\right)\right)}{q(1-D_j)D_j} & \dfrac{C_F L_L\omega_S\omega_L - q^2D_j^2}{q(1-D_j)D_j} \end{bmatrix}$$

$$\left|\underline{H}_U\right| = \left|\frac{\underline{U}_L}{\underline{U}_S}\right| = \left|\frac{1}{\underline{A}_{11} + \underline{A}_{12}/\underline{R}_L}\right|, \quad (35) \qquad \left|\underline{H}_I\right| = \left|\frac{\underline{I}_L}{\underline{I}_S}\right| = \left|\frac{1}{\underline{A}_{22} + \underline{A}_{21}\underline{R}_L}\right|, \quad (36)$$

$$\lambda_S = \frac{P_S}{S_S} = \cos\left[\arg\left(\frac{A_{11}Z_L + A_{12}}{A_{21}Z_L + A_{22}}\right)\right], \quad (37) \qquad \arg|\underline{H}_U| = \arg\left(\frac{1}{\underline{A}_{11} + \underline{A}_{12}/\underline{R}_L}\right). \quad (38)$$

The characteristics of magnitude and phase of voltage transmittance, current transmittance, and input power factor as functions of the load voltage setting frequency and summarized pulse duty factor D_j, obtained by means of (35)-(38) are shown in Fig. 7. Circuit parameters are as follows: U_S -230V/50Hz, f_p=5kHz, {L_{F1}-L_{F3}, L_{S1}-L_{S3}}-2mH, {C_{F1}-C_{F3}, C_{L1}-C_{L3}}-20μF, R_L=10Ω. For purpose of comparison these characteristics are presented together with ones obtained by means of simulation investigations of the presented circuit with idealized switches (Fig. 1). The presented results have been obtained for matching conditions $R_L = \sqrt{L_{Sj}/C_{Lj}} = \sqrt{L_{Fj}/C_{Fj}}$ [8].

As is visible from Fig. 7 properties of the MRFC are strongly dependent on parameters of the passive elements of the discussed circuit. The presented MRFC has the advantageous properties in comparison with the MRFC based on buck-boost and Zeta topology [10]. It has smaller "dispersion" of characteristics as a function of load voltage setting frequency. All characteristics almost ideally coincide for different frequencies of load voltage.

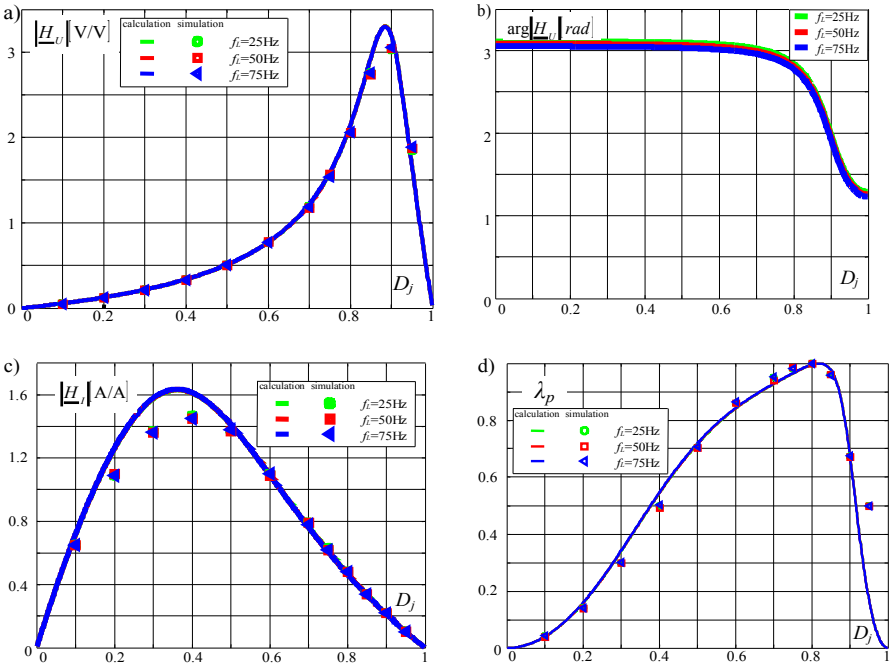

Fig. 7. Steady state characteristics of MRPC based on Ćuk topology as a functions of the load voltage setting frequency and summarized pulse duty factor D_j: a) magnitude of voltage transmittance, b) phase of voltage transmittance, c) magnitude of current transmittance, d) input power factor

5 TRANSIENT-STATE ANALYSIS

The equivalent circuit of transient-state is shown in Fig. 5.

The steady-state averaged state-space equation is described as [19]:

$$\dot{\bar{\mathbf{x}}} \approx \mathbf{A}(D)\bar{\mathbf{x}} + \mathbf{B}(D)\,u_S\,, \tag{39}$$

where $\bar{\mathbf{x}}$ is the vector of the averaged state variables, $\bar{\mathbf{y}}$ is the vector of output variables, D is the duty factor of switch control signal, A(D) is the averaged state matrix, B(D) is the input matrix, C(D) is the output matrix.

For circuits shown in Fig. 5 we obtain the following steady-state averaged state-space equation:

$$\begin{bmatrix} \frac{d\bar{i}_{LF}}{dt} \\ \frac{d\bar{i}_{LS}}{dt} \\ \frac{d\bar{u}_{CF}}{dt} \\ \frac{d\bar{u}_{CL}}{dt} \end{bmatrix} = \begin{bmatrix} -j\omega_S & 0 & -\frac{(1-D_j)}{L_F} & 0 \\ 0 & -j\omega_L & \frac{qD_j}{L_S} & -\frac{1}{L_S} \\ \frac{(1-D_j)}{C_F} & -\frac{qD_j}{C_F} & -j\omega_S & 0 \\ 0 & \frac{1}{C_L} & 0 & -\frac{1}{R_L C_L} - j\omega_L \end{bmatrix} \begin{bmatrix} \bar{i}_{LF} \\ \bar{i}_{LS} \\ \bar{u}_{CF} \\ \bar{u}_{CL} \end{bmatrix} + \begin{bmatrix} \frac{1}{L_F} \\ 0 \\ 0 \\ 0 \end{bmatrix} [u_S]\,. \tag{40}$$

Assuming that all variables have two components: a running constant component (the averaged value in the switching period T_S), which is marked by upper case letter, and a perturbation one marked by lower case letter, which is covered by sign "^":

$$\mathbf{u} = \mathbf{U} + \hat{\mathbf{u}}\,,\ \mathbf{x} = \mathbf{X} + \hat{\mathbf{x}}\,,\ d = D + \hat{d}\,.$$

The small signal state space equations are expressed as follows [19]:

$$\frac{d}{dt}(\mathbf{X} + \hat{\mathbf{x}}) \approx \mathbf{A}\hat{\mathbf{x}} + \mathbf{B}\hat{\mathbf{u}} + [(\mathbf{A}_1 - \mathbf{A}_2)\mathbf{X} + (\mathbf{B})\mathbf{U}]\hat{d}\,, \tag{41}$$

where $\mathbf{A}_1 = \mathbf{A}(D_j = 1, q = 1)$, $\mathbf{A}_2 = \mathbf{A}(D_j = 0, q = 0)$.

According to (41) Laplace transform of a small signal state-space equation is expressed as (42).

$$s\hat{\mathbf{x}}(s) = \mathbf{A}\hat{\mathbf{x}}(s) + \mathbf{B}\hat{\mathbf{u}}(s) + [(\mathbf{A}_1 - \mathbf{A}_2)\mathbf{X} + (\mathbf{B})\mathbf{U}]\hat{d}(s)\,. \tag{42}$$

After rearranging there is:

$$\hat{\mathbf{x}}(s) = (s\mathbf{I} - \mathbf{A})^{-1}\left\{\mathbf{B}\hat{\mathbf{u}}(s) + [(\mathbf{A}_1 - \mathbf{A}_2)\mathbf{X} + (\mathbf{B})\mathbf{U}]\,\hat{d}(s)\right\} = \mathbf{G}_{\hat{u}_L,\hat{\mathbf{u}}}(s)\hat{\mathbf{u}}(s) + \mathbf{G}_{\hat{u}_L,\hat{d}}(s)\,\hat{d}(s)\,, \tag{43}$$

where:

$$\mathbf{G}_{qd0\,\hat{\mathbf{x}},\hat{\mathbf{u}}} = \frac{\hat{\mathbf{x}}_{qd0}(s)}{\hat{\mathbf{u}}_{qd0}(s)}\,, \tag{44}$$

$$\mathbf{G}_{qd0\,\hat{\mathbf{x}},\hat{d}} = \frac{\hat{\mathbf{x}}_{qd0}(s)}{\hat{d}(s)}\,. \tag{45}$$

The transient-state transmittance $\mathbf{G}_{qd0\,\hat{\mathbf{x}},\hat{\mathbf{u}}}$ is defined as:

$$\mathbf{G}_{qd0\hat{\mathbf{x}},\hat{\mathbf{u}}} = \frac{\begin{bmatrix} D_j^2 q^2 \left(1+ R_L C_L \left(s+ j\omega_L\right)\right)+ C_F \left(R_L + L_S \left(1+ R_L C_L \left(s+ j\omega_L\right)\right)\left(s+ j\omega_L\right)\right)\left(s+ j\omega_S\right) \\ \left(D_j - 1\right) D_j q \left(1+ R_L C_L \left(s+ j\omega_L\right)\right) \\ \left(D_j - 1\right)\left(R_L + L_S \left(1+ R_L C_L \left(s+ j\omega_L\right)\right)\left(s- j\omega_L\right)\right) \\ \left(D_j - 1\right) D_j q R_L \end{bmatrix}}{M}, \quad (45)$$

where:

$$M = \left(D_j - 1\right)^2 \left(R_L + L_S \left(1+ R_L C_L \left(s+ j\omega_L\right)\right)\left(s+ j\omega_L\right)\right)+$$
$$+ L_F \left(D_j^2 q^2 \left(1+ R_L C_L \left(s+ j\omega_L\right)\right)+ C_F \left(R_L + L_2 \left(1+ R_L C_L \left(s+ j\omega_L\right)\right)\left(s+ j\omega_L\right)\right)\left(s+ j\omega_S\right)\right)\left(s+ j\omega_S\right).$$

Fig. 8 represent the calculation and simulation test result of transient responses of states variables for two different output frequencies 25 and 75Hz. In both cases the step change of the input voltages from 50% to 100% of their nominal values in time moment t_0 and pulse duty factor equal D_j=0.75 is presented.

In Fig. 9 transient responses of states variables at step change of the output frequency from 25Hz to 50Hz, for summarized pulse duty factor equal D_j=0.75, are presented.

Figures from Fig. 8 to Fig. 9 show good consistency of calculation and simulation test results. Obtained results confirm that small signal models can be useful for transient responses analysis of the described MRFC.

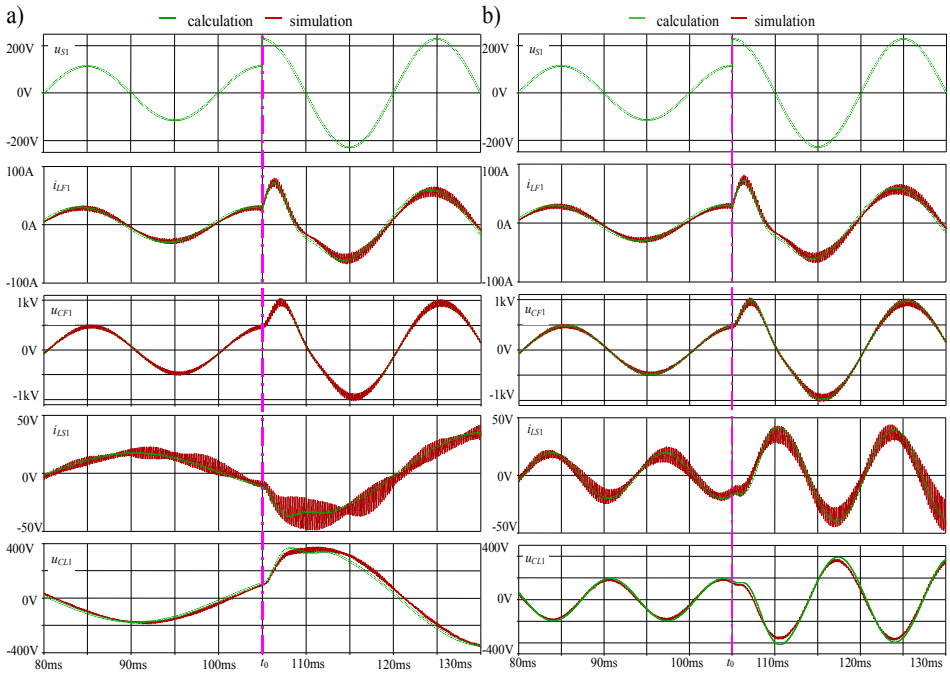

Fig. 8. Transient responses of states variables at step change of the supply voltage: a) f_L=25Hz, b) f_L =75Hz

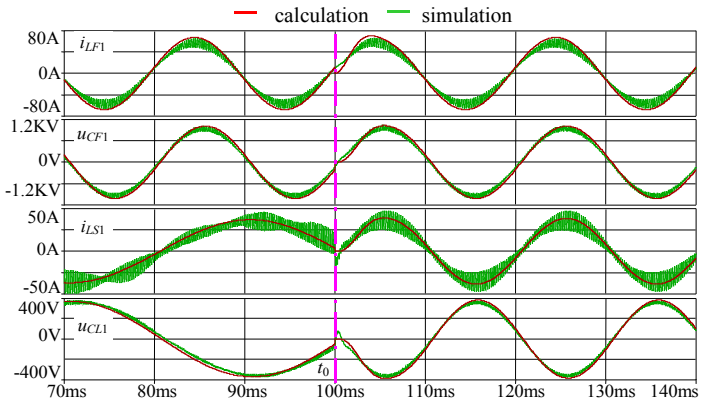

Fig. 9. Transient responses of states variables at step change of the output frequency for D_j=0.75

6 CONCLUSIONS

The steady state and small signal mathematical and circuit models of MRFC with Ćuk topology have been elaborated. Furthermore, the steady state characteristics and transient responses of analysed circuit have been also investigated. Simulation test results, obtained for MRFC with idealized switches, confirmed that elaborated models can be useful to steady state and transient responses of MRFC topology. The validity of proposed models will be the subject of future investigations of presented MRFC with active load and for closed control system as well.

ACKNOWLEDGMENT

This work was supported by the Polish Ministry of Science and Higher Education, Project No N510 036 32/3380.

7 REFERENCES

1. Venturini M., Alesina A.: *The generalized transformer: a new bi-directional sinusoidal waveform frequency converter with continuously adjustable input power factor*, IEEE Power Electronics Specialists Conference Record, PESC'80, pp.242-252.
2. Wheeler P. W., Rodriguez J., Clare J. C., Empringham L., Weinstejn A.: *Matrix converters: A technology review*, IEEE Trans. on Ind. Electronics, Vol.49, No.2, pp.276-288, April 2002.
3. Huber L., Borojevic D.: *Space vector modulated three-phase to three phase matrix converter with input power factor correction*, IEEE Trans. on Ind Appl. Vol.31, No.6, pp.1234-1246, Nov./Dec. 1995.

4. Casadei D., Serra G., Tanti A., Zaroi L.: *Matrix converter modulation strategies: a New general approach based on space-vector representation of switch state*, IEEE Trans. on Ind. Electronics, Vol.49, No.2, pp.370-381, April 2002.
5. Apap M., Clare J. C., Wheeler P. W., Bradley K. J.: *Analysis and comparison of AC-AC Matrix converter control strategies*, Proc. of PESC' 2003, pp.1287-1292, Cairns 2003.
6. Helle L., Larsen K. B., Jorgensen A. H., Munk-Nielsen S., Blaabjerg F.: *Evaluation of modulation schemes for three-phase to three-phase matrix converters*, IEEE Trans. on Ind. Electronics, Vol.51, No.1, pp.158-170, 2004.
7. Zinoviev G. S., Obuchov A. Y., Otchenasch W. A., Popov W. I.: *Transformerless PWM AC boost and buck-boost converters*, (In Russian), Technicznaja Elektrodinamika, T2, pp.36-39. Nacjonalnaja Akademia Nauk Ukrainy, 2000.
8. Fedyczak Z.: *PWM AC voltage transforming circuits,* (In Polish), Oficyna Wydawnicza Uniwersytetu Zielonogórskiego, Zielona Góra, 2003.
9. Fedyczak Z., Szcześniak P.: *Study of matrix-reactance frequency converter with Ćuk topology,* (In Polish), Przegląd Elektrotechniczny, No.7/8, pp.42-47, 2006.
10. Fedyczak Z., Szcześniak P., Kaniewski J.: *Direct PWM AC choppers and frequency converters*, in *Measurements Models Systems and Design*, Charter 16, Wydawnictwa Komunikacji i Łączności, pp.393-424, Warszawa, 2007.
11. Rim C. T., Hu D. Y., Cho G. H.: *Transformers as Equivalent Circuits for Switches: General Proofs and D-Q Transformation – Based Analyses*, IEEE Trans. on Ind. Apl. Vol.26 No.4, 1990.
12. Rim C. T., Choi N. S., Cho G. C., Cho G. H.: *A complete dc and ac analysis of three phase controlled-current PWM rectifier using circuit D-Q transformation*, IEEE Trans. Power Electron., Vol.9, pp.390-396, 1994.
13. Chen J., Ngo D. T.: *Graphical phasor analysis of three-phase PWM converters*, IEEE Trans. On Power Electron., vol.16, No.5, pp.659-666, 2001.
14. Huang X., Chen J., Ngo K. D. T.: *Graphical DC analysis of three-phase PWM converters using a complex transformation*, IEEE International. Symposium on Circuits and Systems, ISCAS 2000, Geneva, vol.3, pp.243-246, 2000.
15. Kwon W. H., Cho G. H.: *Analysis of static and dynamic characteristics of practical step-up nine-switch matrix converter*, Proc. Inst. Elect. Eng. B, vol.140, pp.139-146, 1993.
16. Kwon W. H., Cho G. H.: *Analysis of non-ideal step down matrix converter based on circuit DQ transformation*, IEEE Power Electronics Specialists Conference, PESC'91, Cambridge, USA, pp.825-829, 1991.
17. Fedyczak Z.: *Four-terminal chain parameters of averaged ac models of non-isolated matrix-reactance PWM AC line conditioners*, Archives of Electrical Engineering, Vol.50, No.4, pp.395-409, 2001
18. Osiowski J., Szabatin J.: *Basis of circuits theory,* (in Polish), Vol.3 WNT, Warsaw, 1995
19. Middlebrook R. D., Ćuk S.: *A general unified approach to modelling switching-converter power stages*, PESC'76 Conf. Rec. pp.18-34, 1976.